

Direction Following Control of Planar Snake Robots Using Virtual Holonomic Constraints

Alireza Mohammadi, Ehsan Rezapour, Manfredi Maggiore, and Kristin Y. Pettersen

Abstract—This paper investigates the problem of direction following for planar snake robots. The control objective is to regulate the linear velocity vector of the snake robot to a constant reference while guaranteeing boundedness of the system states. The proposed feedback control strategy enforces virtual constraints encoding a lateral undulatory gait, parametrized by states of dynamic compensators used to regulate the orientation and forward speed of the snake robot.

I. INTRODUCTION

Inspired by biological snakes, snake robots are underactuated vehicle-manipulator systems with many degrees-of-freedom that can effectively be used for operations in challenging environments. The large number of degrees-of-freedom enables snake robots to operate on irregular and cluttered surfaces, to climb stairs, and to even climb on poles. Snake robots pose significant motion control challenges arising from the fact that such robots typically have at least three degrees of underactuation.

One of the basic gait patterns through which biological snakes achieve forward motion is called lateral undulation [1]. During lateral undulation, the snake undergoes periodic shape changes that resemble a wave traveling backward along its body, from head to tail. As a result of this motion, the snake body traces out a periodic curve on the plane, which Hirose [1] mathematically represented as a *serpenoid*. Thinking of a snake robot as a discrete approximation of a biological snake, researchers (see, e.g., [1], [2], [3]) have observed that the serpenoid curve can be well-approximated by imposing the sinusoidal reference signal for the i -th joint angle

$$\phi_{\text{ref},i}(t) = \alpha \sin(\omega t + (i - 1)\delta) + \phi_0, \quad (1)$$

where α denotes the amplitude of the sinusoid, ω denotes the frequency of the joint oscillations, δ denotes the phase shift between two consecutive joints, and ϕ_0 is a joint offset used to control the direction of locomotion.

A. Mohammadi and M. Maggiore were supported by the Natural Sciences and Engineering Research Council (NSERC) of Canada. E. Rezapour and K. Y. Pettersen were partly supported by the Research Council of Norway through the Centres of Excellence funding scheme, project No. 223254 AMOS, and project No. 205622.

A. Mohammadi and M. Maggiore are with the Department of Electrical and Computer Engineering, University of Toronto, 10 King's College Road, Toronto, ON M5S 3G4, Canada. E-mail: alireza.mohammadi@mail.utoronto.ca, maggiore@control.utoronto.ca

E. Rezapour and K. Y. Pettersen are with the Department of Engineering Cybernetics, Norwegian University of Science and Technology, NO-7491 Trondheim, Norway. E-mail: {ehsan.rezapour, Kristin.Y.Pettersen}@itk.ntnu.no

The typical control approach in the snake locomotion literature relies on the asymptotic tracking of suitably designed reference signals, such as (1). In [4], the reference signals are produced by central pattern generators. In [5], path following of a straight line is achieved using the lateral undulatory gait (1) and adapting the joint offset ϕ_0 according to a line-of-sight guidance law. An enhancement of the same technique is presented in [6]. In [7], a careful analysis is presented to generate reference signals to maximize the generation of momentum, with application to path following for a swimming snake robot. In [8], numerical optimal control methods are used to generate gaits. In [9], modal decomposition has been used to modify a snake robot's sidewinding gait to orient the head while locomoting.

In this paper, we propose an approach that removes timed signals entirely from the control loop, and replaces them with state-dependent constraints. Specifically, we replace the time-dependent term ωt in the lateral undulatory gait (1) with the state λ of a compensator, modify the way in which the offset ϕ_0 affects the gait, and view this offset as the state of a second compensator. The result is a state-dependent undulatory gait which can be considered as a dynamic virtual constraint. Virtual constraints have been successfully used in the robot locomotion literature [10], [11] and have been investigated in the general context of Euler-Lagrange control systems [12], [13]. By eliminating exogenous reference signals, virtual constraints enhance the robustness of the feedback loop and add flexibility to the control design.

We investigate the most basic motion control problem of direction following: regulate the velocity of the center of mass of the snake robot to some desired vector while guaranteeing boundedness of the system states. This paper makes two contributions in this direction. First, in addition to controlling the orientation of the snake robot as done, e.g., in [5], [6], we control the entire velocity vector of the center of mass of the robot. Second, we rigorously show that the states of the dynamic compensators used for controlling the orientation and velocity of the snake robot are uniformly bounded. The reason for studying direction following problem is that, as will be shown in future work, this problem is a building block for a more advanced maneuvering problem.

The rest of the paper is organized as follows. In Section II, we present the kinematic and dynamic model of the snake robot. In Section III, we state the control design objectives. In Section IV, we consider the shape control for the robot. In Sections V and VI, we develop control strategies for the head angle and the velocity of the robot, respectively. Finally,

Section VII presents simulation results which illustrate the performance of the proposed control strategy.

Notation. Following the notation in [14], we make use of the following matrices and vectors

$$A = \begin{bmatrix} 1 & 1 & & \\ & \dots & & \\ & & 1 & 1 \\ & & & \dots \end{bmatrix} \in \mathbb{R}^{(N-1) \times N}$$

$$D = \begin{bmatrix} 1 & -1 & & \\ & \dots & & \\ & & 1 & -1 \\ & & & \dots \end{bmatrix} \in \mathbb{R}^{(N-1) \times N}$$

$$e = [1, \dots, 1]^T \in \mathbb{R}^N$$

$$E = \begin{bmatrix} e & 0_{N \times 1} \\ 0_{N \times 1} & e \end{bmatrix} \in \mathbb{R}^{2N \times 2}$$

$$\bar{e} = [1, \dots, 1]^T \in \mathbb{R}^{N-1}, \quad \theta = [\theta_1, \dots, \theta_N]^T \in \mathbb{R}^N$$

$$\sin \theta = [\sin \theta_1, \dots, \sin \theta_N]^T \in \mathbb{R}^N$$

$$\cos \theta = [\cos \theta_1, \dots, \cos \theta_N]^T \in \mathbb{R}^N$$

$$S_\theta = \text{diag}(\sin \theta) \in \mathbb{R}^{N \times N}$$

$$C_\theta = \text{diag}(\cos \theta) \in \mathbb{R}^{N \times N}$$

$$\dot{\theta}^2 = [\dot{\theta}_1^2, \dots, \dot{\theta}_N^2]^T \in \mathbb{R}^N$$

$$b = [0, \dots, 0, 1]^T \in \mathbb{R}^{N-1}$$

$$H = \begin{bmatrix} 1 & 1 & \dots & 1 \\ 0 & 1 & \dots & 1 \\ & \dots & & \\ 0 & 0 & \dots & 1 \\ 0 & 0 & \dots & 0 \end{bmatrix} \in \mathbb{R}^{N \times (N-1)}$$

$$I_N = \begin{bmatrix} 1 & & & \\ & 1 & & \\ & & \dots & \\ & & & 1 \end{bmatrix} \in \mathbb{R}^{N \times N}$$

$$V = A^T (DD^T)^{-1} A$$

$$K = A^T (DD^T)^{-1} D$$

$$SC_\theta = \begin{bmatrix} K^T S_\theta \\ -K^T C_\theta \end{bmatrix}$$

II. MODEL OF THE SNAKE ROBOT

In this section, we review the kinematic and dynamic model of a snake robot presented in [14]. We consider a snake robot with N rigid links each of length $2l$. Each link is assumed to have uniformly distributed mass m and moment of inertia J . We denote the vector of absolute link angles by $\theta = [\theta_1, \dots, \theta_N]^T \in \mathbb{R}^N$, and the center of mass of the robot in inertial coordinates by $p = [p_x, p_y] \in \mathbb{R}^2$. Figure 1 illustrates the kinematic parameters of the snake robot. Table I summarizes the parameters of the snake robot used in our simulations. Following [14], the dynamic equations of the snake robot can be written as follows

$$M_\theta \ddot{\theta} + W_\theta \dot{\theta}^2 - lSC_\theta^T f_R(\theta, \dot{\theta}, \dot{p}) = D^T u, \quad (2a)$$

$$Nm\ddot{p} = E^T f_R(\theta, \dot{\theta}, \dot{p}), \quad (2b)$$

where $u \in \mathbb{R}^{N-1}$ is the vector of actuator torques, f_R is the vector of ground friction forces, and the remaining quantities are defined as follows:

$$M_\theta = JI_N + ml^2 S_\theta V S_\theta + ml^2 C_\theta V C_\theta, \quad (3a)$$

$$W_\theta = ml^2 S_\theta V C_\theta - ml^2 C_\theta V S_\theta. \quad (3b)$$

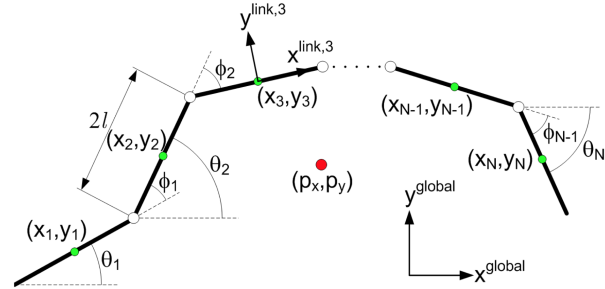


Fig. 1. Kinematic parameters of the snake robot.

TABLE I
THE PARAMETERS OF THE SNAKE ROBOT

Symbol	Description	Numerical values in simulations
N	Number of links.	10
$2l$	Length of a link.	0.14 m
m	Mass of a link.	1 kg
$\theta \in \mathbb{R}^N$	Vector of absolute link angles.	-
$\phi \in \mathbb{R}^{N-1}$	Vector of joint angles.	-
$p = [p_x, p_y] \in \mathbb{R}^2$	CM position of the robot.	-
c_t	Tangential viscous friction coefficient.	0.1
c_n	Normal viscous friction coefficient.	1

The mechanical system (2a)-(2b) has $n + 2$ configuration variables and $n - 1$ controls. It therefore has three degrees of underactuation. The actuator torques have no direct effect on the centre of mass dynamics (2b). The only coupling between joint dynamics (2a) and centre of mass dynamics (2b) occurs through the ground friction force f_R . This coupling is the essential mechanism underlying snake locomotion, and it is what makes the motion control problem challenging.

For simplicity, we assume that the friction forces acting on the robot are viscous. A snake robot which is subject to viscous friction qualitatively (although not quantitatively) behaves similar to a snake robot which is subject to Coulomb friction force [14]. We have:

$$\begin{aligned} f_R(\theta, \dot{\theta}, \dot{p}) &= \begin{bmatrix} f_{R,x} \\ f_{R,y} \end{bmatrix} = Q_\theta \begin{bmatrix} \dot{X} \\ \dot{Y} \end{bmatrix} \\ &= Q_\theta \begin{bmatrix} lK^T S_\theta \dot{\theta} + e\dot{p}_x \\ -lK^T C_\theta \dot{\theta} + e\dot{p}_y \end{bmatrix} = lQ_\theta SC_\theta \dot{\theta} + Q_\theta E\dot{p} \end{aligned}$$

where $X = [x_1, \dots, x_N] \in \mathbb{R}^N$, $Y = [y_1, \dots, y_N] \in \mathbb{R}^N$ are the vectors of inertial coordinates of the centers of mass of the links of the robot. The matrix Q_θ maps the inertial frame velocities of the centers of mass of the links to the

inertial frame viscous friction forces acting on the links, and it is given by

$$Q_{\theta} = - \begin{bmatrix} c_t(C_{\theta})^2 + c_n(S_{\theta})^2 & (c_t - c_n)S_{\theta}C_{\theta} \\ (c_t - c_n)S_{\theta}C_{\theta} & c_t(S_{\theta})^2 + c_n(C_{\theta})^2 \end{bmatrix}, \quad (4)$$

where c_t and c_n denote the tangential and normal viscous friction coefficients of the links, respectively.

Finally, letting $u_{\theta_N} = [\cos \theta_N, \sin \theta_N]^T$ and $v_{\theta_N} = [-\sin \theta_N, \cos \theta_N]^T$, we define

$$v_t = u_{\theta_N}^T \dot{p}, \quad (5a)$$

$$v_n = v_{\theta_N}^T \dot{p}. \quad (5b)$$

The scalars v_t and v_n defined above are the components of the inertial velocity of the center of mass parallel and perpendicular to the angle of the head, respectively.

III. CONTROL DESIGN OBJECTIVES

In this section we present the blueprint of our control design. We begin by stating the control specification.

Direction Following Problem (DFP): Given a desired constant velocity vector \dot{p}_{ref} with polar representation $(r, \theta) = (v_{\text{ref}}, \theta_{\text{ref}})$, design a smooth feedback controller achieving the following specifications:

- (i) Practical stabilization of the head angle θ_N to θ_{ref} .
- (ii) Practical stabilization of the tangential velocity $v_t = u_{\theta_N}^T \dot{p}$ to v_{ref} .
- (iii) Uniform ultimate boundedness of the normal velocity $v_n = v_{\theta_N}^T \dot{p}$ with a small ultimate bound, and ultimate boundedness of the joint dynamics and all controller states.

The above problem formulation relies on the observation that if $\theta_N = \theta_{\text{ref}}$, then making $\dot{p} \rightarrow \dot{p}_{\text{ref}}$ is equivalent to making $(v_t, v_n) \rightarrow (v_{\text{ref}}, 0)$.

Solution Methodology:

In order to solve the DFP, we stabilize a lateral undulatory gait for the shape variables of the robot. Our approach unfolds in three stages.

Stage 1: Shape Control. We use the controls u in (2a) to stabilize a virtual constraint encoding a lateral undulatory gait similar to (1), in which ωt is replaced by a state λ , and ϕ_0 affects only the head angle θ_N . The evolution of λ, ϕ_0 is governed by two compensators, $\dot{\phi}_0 = u_{\phi_0}$ and $\ddot{\lambda} = u_{\lambda}$.

Stage 2: Head Angle Control. Inspired by the biological observation that snakes keep their head pointed towards a target while their body undulates behind the head, we design u_{ϕ_0} to practically stabilize $\theta_N \rightarrow \theta_{\text{ref}}$ while guaranteeing that $(\phi_0, \dot{\phi}_0)$ is uniformly ultimately bounded.

Stage 3: Velocity regulation. We design u_{λ} to practically stabilize $v_t \rightarrow v_{\text{ref}}$ while guaranteeing that v_n settles into a small neighborhood of the origin and $\dot{\lambda}$ is uniformly ultimately bounded.

Figure 2 depicts the structure of the proposed direction following controller.

IV. SHAPE CONTROL

In this section, we use the control inputs u in (2a) to stabilize the lateral undulatory gait for the shape variables of the robot. Inspired by the lateral undulatory gait, we stabilize the relations:

$$\theta_i - \theta_{i+1} = \alpha \sin(\lambda + (i-1)\delta), \quad i = 1, \dots, N-2, \quad (6a)$$

$$\theta_{N-1} - \theta_N = \alpha \sin(\lambda + (N-2)\delta) + \phi_0, \quad (6b)$$

where (α, δ) are positive constants referred to as gait parameters and $(\lambda, \phi_0) \in S^1 \times \mathbb{R}$ are the states of two compensators

$$\ddot{\lambda} = u_{\lambda}, \quad \ddot{\phi}_0 = u_{\phi_0}, \quad (7)$$

to be designed later. The relations (6a)–(6b) are referred to as virtual holonomic constraints (VHC) [12], [13], and they have the property that they can be made invariant through feedback control. These VHCs are parametrized by the states of the dynamic compensators in (7).

Let $\Phi_i(\lambda) = \alpha \sin(\lambda + (i-1)\delta)$, $i = 1, \dots, N-1$ and $\Phi(\lambda) = [\Phi_1(\lambda), \dots, \Phi_{N-1}(\lambda)]^T \in \mathbb{R}^{N-1}$. Since $\theta = HD\theta + e\theta_N$, the relations in (6a)–(6b) can be expressed in vector form as follows:

$$\theta = e\theta_N + H\Phi(\lambda) + Hb\phi_0. \quad (8)$$

The above can also be written as $h(\lambda, \phi_0, \theta) = 0$, where

$$h(\lambda, \phi_0, \theta) = D\theta - \Phi(\lambda) - b\phi_0. \quad (9)$$

If we view $h(\lambda, \phi_0, \theta)$ as an output function for system (2) augmented with compensators (7), then this output yields a vector relative degree $\{2, \dots, 2\}$ everywhere because $\text{rank}(DM_{\theta}^{-1}D^T) = N-1$. Consequently, the zero dynamics manifold associated with output (9) is the set

$$\Gamma = \{(\theta, \dot{\theta}, p, \dot{p}, \lambda, \dot{\lambda}, \phi_0, \dot{\phi}_0) \in \mathbb{R}^{2N+8} : D\theta = \Phi(\lambda) + b\phi_0, D\dot{\theta} = \Phi'(\lambda)\dot{\lambda} + b\dot{\phi}_0\}.$$

We refer to Γ as the constraint manifold associated with the VHC (6). Stabilizing the VHC (6) corresponds to stabilizing Γ . To this end, we use the input-output linearizing control law

$$\begin{aligned} u &= (DM_{\theta}^{-1}D^T)^{-1} \{DM_{\theta}^{-1}W_{\theta}\dot{\theta}^2 \\ &\quad - lDM_{\theta}^{-1}SC_{\theta}^T f_R + \Phi''(\lambda)\dot{\lambda}^2 + \Phi'(\lambda)u_{\lambda} \\ &\quad + bu_{\phi_0} - K_P[D\theta - \Phi(\lambda) - b\phi_0] \\ &\quad - K_D[D\dot{\theta} - \Phi'(\lambda)\dot{\lambda} - b\dot{\phi}_0]\}, \end{aligned} \quad (10)$$

where K_D, K_P are positive definite diagonal matrices containing the joint controller gains. After asymptotically stabilizing Γ , we are left with two control inputs, $(u_{\lambda}, u_{\phi_0})$ to solve the direction following problem. In particular, we use the dynamic compensators to regulate the head angle and the velocity of the robot to desired values. To this end, we first derive the reduced dynamics of the robot, i.e., we reduce the system to the invariant manifold Γ . By left multiplying

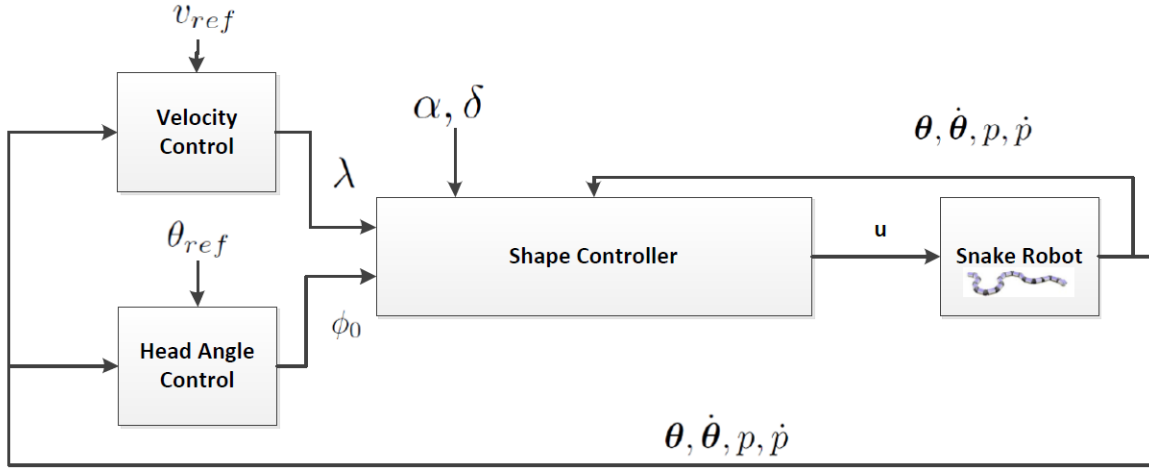


Fig. 2. The structure of the direction following controller.

both sides of (2a) by e^T , which is a left annihilator of the control input matrix D^T , and evaluating the result on the virtual constraint manifold Γ , the dynamics of the snake robot on the virtual constraint manifold Γ read as

$$\ddot{\theta}_N = \Psi_1(\theta_N, \dot{\theta}_N, \lambda, \dot{\lambda}, \phi_0, \dot{\phi}_0, p, \dot{p}) + \Psi_2(\theta_N, \lambda, \phi_0)u_\lambda + \Psi_3(\theta_N, \lambda, \phi_0)u_{\phi_0}, \quad (11a)$$

$$\ddot{p} = \Psi_4(\theta_N, \lambda, \phi_0)\dot{p} + \Psi_5(\theta_N, \lambda, \phi_0)\dot{\theta}_N + \Psi_6(\theta_N, \lambda, \phi_0)\dot{\lambda} + \Psi_7(\theta_N, \lambda, \phi_0)\dot{\phi}_0, \quad (11b)$$

$$\ddot{\phi}_0 = u_{\phi_0}, \quad (11c)$$

$$\ddot{\lambda} = u_\lambda, \quad (11d)$$

where

$$\Psi_1(\cdot) = -\frac{e^T M_\theta H \Phi''(\lambda)}{e^T M_\theta e} \dot{\lambda}^2 - \frac{1}{e^T M_\theta e} \{W_\theta \dot{\theta}^2 - l S C_\theta^T f_R\}, \quad (12a)$$

$$\Psi_2(\cdot) = -\frac{e^T M_\theta H \Phi'(\lambda)}{e^T M_\theta e}, \quad (12b)$$

$$\Psi_3(\cdot) = -\frac{e^T M_\theta H b}{e^T M_\theta e}, \quad (12c)$$

$$\Psi_4(\cdot) = \frac{1}{Nm} E^T Q_\theta E, \quad (12d)$$

$$\Psi_5(\cdot) = \frac{l}{Nm} E^T Q_\theta S C_\theta e, \quad (12e)$$

$$\Psi_6(\cdot) = \frac{l}{Nm} E^T Q_\theta S C_\theta H \Phi'(\lambda), \quad (12f)$$

$$\Psi_7(\cdot) = \frac{l}{Nm} E^T Q_\theta S C_\theta H b. \quad (12g)$$

In the above, each $\Psi_i(\cdot)$ is evaluated on the constraint manifold Γ . The equations in (11) describe a control system with two inputs, (u_{ϕ_0}, u_λ) . This system completely describes the motion of the snake once the VHC (6) has been enforced. The control specification for system (11) is to stabilize θ_N to an arbitrarily small neighborhood of θ_{ref} ; to stabilize $v_t =$

$u_{\theta_N}^T \dot{p}$ to an arbitrarily small neighborhood of v_{ref} ; and finally, to guarantee that $v_n = v_{\theta_N}^T \dot{p}$ goes to a neighborhood of the origin. Meanwhile, we also require $(\dot{\lambda}, \phi_0, \dot{\phi}_0)$ to remain bounded. In the process of developing controllers for the reduced dynamics system, we will require some knowledge of each $\Psi_i(\cdot)$ which is summarized in the following remark.

Remark 4.1: We make some numerical observations that are important in the subsequent development of our control laws. It can be numerically verified that for all gait parameters (α, δ) : (a) $\Psi_3(\cdot) = -e^T M_\theta H b / e^T M_\theta e$ is bounded away from zero and negative for all $\theta_N, \lambda, \phi_0$; (b) $v_{\theta_N}^T \Psi_4(\cdot) v_{\theta_N} \approx -c_n / m$ for all $\theta_N, \lambda, \phi_0$; (c) There exists $\gamma_6 > 0$ such that $-u_{\theta_N}^T \Psi_6(\cdot) < -\gamma_6$ for all θ_N, λ and small values of ϕ_0 and for $c_n > c_t$; (d) There exists $\epsilon_0 > 0$ such that we have $|v_{\theta_N}^T \Psi_6(\cdot)| \leq \alpha \epsilon_0$ for all $\theta_N, \lambda, \phi_0$ where α denotes the amplitude of sinusoidal joint motion in (6a)–(6b); (e) $\|\Psi_4(\cdot)\| \leq c_n / m$ for all $\theta_N, \lambda, \phi_0$; (f) There exists $\gamma_7 > 0$ such that $\|\Psi_7(\cdot)\| \leq \gamma_7$ for all $\theta_N, \lambda, \phi_0$; (g) $|v_{\theta_N}^T \Psi_4(\cdot) u_{\theta_N}| < c_t / m$ for all $\theta_N, \lambda, \phi_0$. Note that the above observations are independent of the parameters N, m, l, J . \triangle

V. HEAD ANGLE CONTROL

In this section, we consider the head angle control for the snake robot. Using the control input u_{ϕ_0} , we control the head angle of the snake robot by controlling the states $(\theta_N, \dot{\theta}_N, \phi_0, \dot{\phi}_0)$ of the constrained system (11a)–(11c). In order to do so, we design a high-gain feedback $u_{\phi_0}(\theta_N, \dot{\theta}_N, \phi_0, \dot{\phi}_0)$ that makes $(\theta_N - \theta_{ref}, \dot{\theta}_N)$ converge to an arbitrarily small neighborhood of the origin and $(\phi_0, \dot{\phi}_0)$ uniformly ultimately bounded. This analysis is made independent of the choice of u_λ , using time scale separation. By (11a) and (11c), the dynamic equations governing the states $(\theta_N, \dot{\theta}_N, \phi_0, \dot{\phi}_0)$ of the constrained system can be written as

$$\begin{aligned} \ddot{\theta}_N &= f_1(\theta_N, \dot{\theta}_N, \lambda, \dot{\lambda}, \phi_0, \dot{\phi}_0, u_\lambda) + \Psi_3(\cdot)u_{\phi_0}, \\ \ddot{\phi}_0 &= u_{\phi_0}. \end{aligned} \quad (13)$$

Proposition 5.1: Consider the head angle control law for system (13)

$$u_{\phi_0} = \frac{1}{\epsilon} \left[\dot{\theta}_N + k_N(\theta_N - \theta_{\text{ref}}) \right] - k_1 \phi_0 - k_2 \dot{\phi}_0. \quad (14)$$

Also, assume that $u_\lambda(t), \dot{\lambda}(t)$ are defined for all $t \geq 0$. Then for any $k_N, k_1, k_2 > 0$, there exist $\epsilon^*, k > 0$ such that for all $\epsilon \in (0, \epsilon^*)$

$$\limsup_{t \rightarrow +\infty} |\theta_N(t) - \theta_{\text{ref}}| = k\epsilon \quad (15)$$

$$\limsup_{t \rightarrow +\infty} |\dot{\theta}_N(t)| = k\epsilon. \quad (16)$$

Moreover, the states $(\phi_0, \dot{\phi}_0)$ are uniformly ultimately bounded.

Remark 5.2: Under (14), the head angle error can be made arbitrarily small provided that ϵ is chosen to be sufficiently small. \triangle

Remark 5.3: In the next section we define a feedback controller u_λ guaranteeing that for any initial condition, the closed-loop system has no finite escape times (see Remark 6.1). This will guarantee that the above proposition is applicable. \triangle

Proof: Viewing the states $\lambda(t), \dot{\lambda}(t)$, and the input $u_\lambda(t)$ as exogenous signals, the control system (13) can be viewed as a time-varying system with states $(\theta_N, \dot{\theta}_N, \phi_0, \dot{\phi}_0)$. Under the control input (14), the closed-loop dynamics of system (13) in the standard singular perturbation form become

$$\begin{aligned} \dot{\theta}_N &= \omega_N, \\ \epsilon \dot{\omega}_N &= \epsilon [g_1(t, \phi_0, \dot{\phi}_0, \theta_N, \dot{\theta}_N) - k_1 \phi_0 - k_2 \dot{\phi}_0] \\ &\quad + \Psi_3(\cdot)(\dot{\omega}_N + k_N \Delta \theta_N), \end{aligned} \quad (17)$$

where

$$g_1(t, \phi_0, \dot{\phi}_0, \theta_N, \dot{\theta}_N) = f_1(\theta_N, \dot{\theta}_N, \lambda(t), \dot{\lambda}(t), \phi_0, \dot{\phi}_0, u_\lambda(t)).$$

Here we use time-scale separation to make the analysis independent of the choice of u_λ . Note that (17) is a singularly perturbed system with reduced dynamics

$$\Delta \dot{\theta}_N = -k_N \Delta \theta_N, \quad (18)$$

where $\Delta \theta_N = \theta_N - \theta_{\text{ref}}$, and boundary-layer dynamics

$$\frac{dy}{d\tau} = \Psi_3(\cdot)y, \quad (19)$$

where $y = \omega_N + k_N \Delta \theta_N$. The origin is an exponentially stable equilibrium point of the reduced system. Also, the origin is an exponentially stable equilibrium point of the boundary-layer system because, by Remark 4.1(a), for some $\gamma_0 > 0$, $\Psi_3(\cdot) \leq -\gamma_0 < 0$ uniformly in t . According to the singular perturbation theorem on an infinite interval (see Theorem 11.2 in [15]), for all $\xi_0, y_0 \in \mathbb{R}$ and $t_0 \geq 0$, the singularly perturbed system (17) has a unique solution $(\Delta \theta_N(t, \epsilon), \omega_N(t, \epsilon))$ such that

$$\begin{aligned} \Delta \theta_N(t, \epsilon) &= \exp(-k_N(t - t_0))(\xi_0 - \theta_{\text{ref}}) \\ &= O(\epsilon), \end{aligned} \quad (20a)$$

$$\begin{aligned} \omega_N(t, \epsilon) &= k_N \exp(-k_N(t - t_0))(\xi_0 - \theta_{\text{ref}}) \\ &\quad - \exp\left(\int_{t_0}^{t/\epsilon} \Psi_3(\cdot) d\tau\right) y_0 = O(\epsilon), \end{aligned} \quad (20b)$$

for all $t \in (0, \infty)$. This proves the first part of the proposition. For the second part, note that the closed-loop dynamics governing the states $(\phi_0, \dot{\phi}_0)$ become

$$\ddot{\phi}_0 + k_2 \dot{\phi}_0 + k_1 \phi_0 = \underbrace{\frac{1}{\epsilon}(\omega_N(t, \epsilon) + k_N \Delta \theta_N(t, \epsilon))}_{f_N(t, \epsilon)}. \quad (21)$$

From (20a)–(20b), it can be seen that $f_N(t, \epsilon)$ is uniformly bounded and of order $O(1)$. Since the unforced system $\ddot{\phi}_0 + k_2 \dot{\phi}_0 + k_1 \phi_0 = 0$ is an LTI system and has a globally exponentially stable equilibrium point at the origin $(\phi_0, \dot{\phi}_0) = (0, 0)$, the system (21) is input-to-state stable. This proves the second part of the proposition. \blacksquare

VI. VELOCITY CONTROL

Consider the reduced dynamics (11). In the previous section, we controlled the states $\theta_N, \dot{\theta}_N, \phi_0, \dot{\phi}_0$. Now, we are left with the states $p, \dot{p}, \lambda, \dot{\lambda}$. The map $\dot{p} \mapsto (v_t, v_n)$ is a diffeomorphism so for velocity control we may consider the subsystem with states $(\Delta v_t, v_n, \lambda, \dot{\lambda})$, with $\Delta v_t = v_t - v_{\text{ref}}$. In order to obtain the tangential and normal velocity dynamics, we take the time derivatives of equations (5a), (5b), which using (11b) yields

$$\begin{aligned} \dot{v}_t &= u_{\theta_N}^T \Psi_4(\cdot) u_{\theta_N} v_t + u_{\theta_N}^T \Psi_4(\cdot) v_{\theta_N} v_n + \dot{\theta}_N v_n + \\ &\quad u_{\theta_N}^T \Psi_5(\cdot) \dot{\theta}_N + u_{\theta_N}^T \Psi_6(\cdot) \dot{\lambda} + u_{\theta_N}^T \Psi_7(\cdot) \dot{\phi}_0 \end{aligned} \quad (22a)$$

$$\begin{aligned} \dot{v}_n &= v_{\theta_N}^T \Psi_4(\cdot) u_{\theta_N} v_t + v_{\theta_N}^T \Psi_4(\cdot) v_{\theta_N} v_n - \dot{\theta}_N v_t + \\ &\quad v_{\theta_N}^T \Psi_5(\cdot) \dot{\theta}_N + v_{\theta_N}^T \Psi_6(\cdot) \dot{\lambda} + v_{\theta_N}^T \Psi_7(\cdot) \dot{\phi}_0. \end{aligned} \quad (22b)$$

Thus, the velocity error dynamics have the form

$$\begin{aligned} \Delta \dot{v}_t &= f_2(\theta_N, \dot{\theta}_N, \lambda, \dot{\lambda}, \phi_0, \dot{\phi}_0, \Delta v_t, v_n) + \\ &\quad u_{\theta_N}^T \Psi_6(\cdot) \dot{\lambda}, \end{aligned} \quad (23a)$$

$$\begin{aligned} \dot{v}_n &= f_3(\theta_N, \dot{\theta}_N, \lambda, \dot{\lambda}, \phi_0, \dot{\phi}_0, \Delta v_t, v_n) + \\ &\quad v_{\theta_N}^T \Psi_4(\cdot) v_{\theta_N} v_n, \end{aligned} \quad (23b)$$

$$\ddot{\lambda} = u_\lambda. \quad (23c)$$

In order to stabilize the solutions of (23a), (23b) to a neighborhood of the origin, we iteratively introduce control-Lyapunov functions (CLF) using the techniques of backstepping [16]. To this end, we start by defining the first CLF in the form

$$V_1 = \frac{1}{2} \Delta v_t^2, \quad (24)$$

and taking its time derivative along the solutions of (23a) to obtain

$$\dot{V}_1 = \Delta v_t \Delta \dot{v}_t = \Delta v_t (u_{\theta_N}^T \Psi_6(\cdot) \dot{\lambda} + f_2(\cdot)). \quad (25)$$

We use $\dot{\lambda}$ as a virtual control input by defining $\dot{\lambda}$ equal to $-k_\lambda \Delta v_t$ for some positive constant k_λ . We introduce the error variable

$$z = \dot{\lambda} + k_\lambda \Delta v_t, \quad (26)$$

that we would like to drive to zero, and re-write (25) as

$$\dot{V}_1 = -k_\lambda u_{\theta_N}^T \Psi_6(\cdot) (\Delta v_t)^2 + \Delta v_t u_{\theta_N}^T \Psi_6(\cdot) z + \Delta v_t f_2(\cdot). \quad (27)$$

To perform backstepping for z , we define a composite CLF in the form

$$V_2 = V_1 + \frac{1}{2} z^2 + \frac{1}{2} v_n^2. \quad (28)$$

Taking the time derivative of (28) along the solutions of (23a)-(23c), we have

$$\begin{aligned} \dot{V}_2 &= -u_{\theta_N}^T \Psi_6(\cdot) k_\lambda \Delta v_t^2 + z(u_\lambda + k_\lambda \Delta v_t) \\ &+ \Delta v_t u_{\theta_N}^T \Psi_6(\cdot) + v_{\theta_N}^T \Psi_4(\cdot) v_{\theta_N} v_n^2 + v_n (f_3 - v_{\theta_N}^T \Psi_6(\cdot) \dot{\lambda}) \\ &+ v_n v_{\theta_N}^T \Psi_6(\cdot) (z - k_\lambda \Delta v_t). \end{aligned} \quad (29)$$

In order to achieve the velocity control objective, we define the feedback controller

$$\begin{aligned} u_\lambda &= -k_\lambda \underbrace{\{f_2(\cdot) + u_{\theta_N}^T \Psi_6(\cdot) \dot{\lambda}\}}_{\Delta \dot{v}_t} - K_z z \\ &- \Delta v_t u_{\theta_N}^T \Psi_6(\cdot) - v_n v_{\theta_N}^T \Psi_6(\cdot). \end{aligned} \quad (30)$$

Remark 6.1: Consider the state vector $x = [v_t, v_n, \lambda, \dot{\lambda}, \phi_0, \dot{\phi}_0]^T$. Under the control laws (14) and (30), we have $\dot{x} = f(x)$ for the closed loop system. Because of the uniform bounds on $\Psi_i, i = 2, \dots, 7$, it can be seen that $\|f(x)\| \leq B(1 + \|x\|)$ for some constant B . Because of this linear growth condition, there is no finite escape time and the signals $\dot{\lambda}(t), u_\lambda(t)$ are defined for all $t \geq 0$ as required by Proposition 5.1. \triangle

We have the following proposition regarding the velocity control system.

Proposition 6.2: Consider the control system (23a)-(23c) under the controller (30). If the ultimate bound on ϕ_0 from Proposition 5.1 is small enough such that $u_{\theta_N}^T \Psi_6(\cdot)$ is bounded away from zero, then for all $\epsilon > 0$, there exists a controller gain $k_\lambda > 0$ and positive constants α^*, c^* such that, for all $\alpha \in (0, \alpha^*)$ and all $c_n - c_t > c^*$, the set $\Gamma' = \{(\lambda, \dot{\lambda}, v_t, v_n) \mid |\Delta v_t| < \epsilon\}$ is asymptotically stable. Moreover, $\dot{\lambda}$ and v_n are uniformly ultimately bounded.

Remark 6.3: Under (30), the velocity error Δv_t can be made arbitrarily small provided that the gain k_λ is chosen to be sufficiently large. \triangle

Proof: Substituting (30) into (29) yields

$$\begin{aligned} \dot{V}_2 &= -u_{\theta_N}^T \Psi_6(\cdot) k_\lambda \Delta v_t^2 - K_z z^2 + v_{\theta_N}^T \Psi_4(\cdot) v_{\theta_N} v_n^2 \\ &+ v_n (f_3(\cdot) - v_{\theta_N}^T \Psi_6(\cdot) \dot{\lambda}) - k_\lambda v_n v_{\theta_N}^T \Psi_6(\cdot) \Delta v_t \end{aligned} \quad (31)$$

Therefore, by parts (b) and (c) of Remark 4.1, we have, for small enough ϕ_0 ,

$$\begin{aligned} \dot{V}_2 &\leq -\gamma_6 k_\lambda \Delta v_t^2 - K_z z^2 - \frac{c_n}{m} v_n^2 + v_n \\ &\cdot \underbrace{(v_{\theta_N}^T \Psi_4(\cdot) u_{\theta_N} \Delta v_t + v_{\theta_N}^T \Psi_7(\cdot) \dot{\phi}_0 + v_{\theta_N}^T \Psi_4(\cdot) u_{\theta_N} v_{\text{ref}})}_{f_3(\cdot) - v_{\theta_N}^T \Psi_6(\cdot) \dot{\lambda}} \\ &- k_\lambda v_n v_{\theta_N}^T \Psi_6(\cdot) \Delta v_t \end{aligned} \quad (32)$$

By Proposition 5.1, $\dot{\phi}_0$ is uniformly ultimately bounded by δ_{ϕ_0} . By parts (d), (e), (f), (g) of Remark 4.1, we have $\|\Psi_4\| \leq c_n/m$, $\|\Psi_7\| \leq \gamma_7$, $|v_{\theta_N}^T \Psi_4 u_{\theta_N}| < c_t/m$, and $|v_{\theta_N}^T \Psi_6(\cdot)| \leq \alpha \epsilon_0$, and thus

$$\begin{aligned} \dot{V}_2 &\leq -\gamma_6 k_\lambda \Delta v_t^2 - K_z z^2 - \frac{c_n}{m} v_n^2 \\ &+ \frac{c_t}{m} |v_n| |\Delta v_t| + \gamma_7 |v_n| |\dot{\phi}_0| + \\ &\frac{c_n}{m} v_{\text{ref}} |v_n| + k_\lambda \epsilon_0 |v_n| |\Delta v_t|. \end{aligned} \quad (33)$$

Using the fact that, for any $\gamma > 0$, $ab \leq (\gamma/2)a^2 + (1/2\gamma)b^2$, we have

$$\begin{aligned} \dot{V}_2 &\leq - \left[k_\lambda \gamma_6 - \frac{1}{2} \left(\frac{c_t}{m} + k_\lambda \alpha \epsilon_0 \right) \right] \Delta v_t^2 - K_z z^2 \\ &- \left[\frac{c_n}{m} - \left(\frac{c_t}{m} + k_\lambda \alpha \epsilon_0 \right) \frac{1}{2} - \frac{\gamma_7 \gamma}{2} - \frac{c_n \gamma'}{2m} \right] v_n^2 + \frac{\gamma_7}{2\gamma} \delta_{\phi_0}^2 \\ &+ \frac{c_n}{2m\gamma'} v_{\text{ref}}^2, \end{aligned} \quad (34)$$

where γ and γ' are arbitrary positive numbers. Pick $\alpha < \gamma_6/\epsilon_0$ and $k_\lambda > c_t/(m\gamma_6)$. Then, the coefficient premultiplying Δv_t^2 in (34) is negative. Moreover, if $c_n > (c_t/2) + mk_\lambda \gamma_6$, then for sufficiently small $\gamma, \gamma' > 0$, the coefficient of v_n^2 in (34) is also negative. In conclusion, for sufficiently large $c_n - c_t$ and k_λ , and sufficiently small α , there exists $\beta > 0$ such that

$$\dot{V}_2 \leq -\beta V_2 + \frac{\gamma_7}{2\gamma} \delta_{\phi_0}^2 + \frac{c_n}{2m\gamma'} v_{\text{ref}}^2, \quad (35)$$

from which it follows, by the comparison lemma [15], that

$$\begin{aligned} V_2(t) &\leq V_2(0) \exp(-\beta t) + \\ &(\frac{\gamma_7}{2\gamma} \delta_{\phi_0}^2 + \frac{c_n}{2m\gamma'} v_{\text{ref}}^2) / (\beta). \end{aligned} \quad (36)$$

This implies that the solutions of (23a)-(23c), i.e., $\Delta v_t, v_n, \dot{\lambda}$, remain bounded, V_2 converges to a ball of radius $(\frac{\gamma_7}{2\gamma} \delta_{\phi_0}^2 + \frac{c_n}{2m\gamma'} v_{\text{ref}}^2) / (\beta)$, and therefore $\|[\Delta v_t, v_n, \dot{\lambda}]^T\|$ converges to a neighborhood of the origin given by $\sqrt{(\frac{\gamma_7}{2\gamma} \delta_{\phi_0}^2 + \frac{c_n}{2m\gamma'} v_{\text{ref}}^2) / (2\beta)}$.

Moreover, we can use the first CLF, i.e., $V_1 = 1/2 \Delta v_t^2$, to show the practical stability of the tangential velocity. Taking its time derivative along the solutions of (23a)-(23c) given in (27) and using the fact that $u_{\theta_N}^T \Psi_6$ is uniformly bounded we have

$$\dot{V}_1 \leq -k_\lambda \gamma_6 \Delta v_t^2 + \Upsilon_6 |\Delta v_t| |z| + |\Delta v_t| |f_2(\cdot)| \quad (37)$$

By the previous argument, $|z|$ is ultimately bounded. Also, there exists δ_2 such that $\|f_2(\cdot)\| < \delta_2$, so that

$$\dot{V}_1 \leq -(k_\lambda \gamma_6 - \frac{\Upsilon_6}{2} - \frac{1}{2}) \Delta v_t^2 + \underbrace{\frac{\Upsilon_6}{2} \delta_z^2 + \frac{1}{2} \delta_2^2}_d. \quad (38)$$

For sufficiently large k_λ , there exists $\beta > 0$ such that

$$\dot{V}_1 \leq -2\beta V_1 + d, \quad (39)$$

from which we get

$$V_1(t) \leq \exp(-2\beta t) V_1(0) + \frac{1}{2\beta} d, \quad t \geq 0. \quad (40)$$

Therefore, Δv_t converges to a ball of radius $\sqrt{\frac{1}{\beta} d}$. Since $\beta = k_\lambda \gamma_6 - \frac{\Upsilon_6 \gamma}{2} - \frac{1}{2}$, choosing k_λ large enough makes the ultimate bound of Δv_t less than ϵ for any desired $\epsilon > 0$. ■

VII. SIMULATION RESULTS

In this section, we present the simulation results which illustrate the performance of the proposed direction following controller. We considered a snake robot with $N = 10$ links with length $2l = 0.14$ m, mass $m = 1$ kg, and moment of inertia $J = 0.0016$ kg.m². The friction coefficients were $c_t = 0.1$ and $c_n = 1$. The parameters of the VHC were chosen to be $\alpha = 30\pi/180$ rad, and $\delta = 72\pi/180$ rad. We would like to regulate the velocity of the center of mass of the robot to $[-0.0354 \ -0.0354]^T$, i.e., the reference head angle is taken to be $-\pi/4$ rad and $v_{\text{ref}} = 5$ cm/s. The controller parameters were chosen to be $k_p = 100, k_d = 10$ in (10), $\epsilon = 10^{-4}, k_N = 10, k_1 = 1, k_2 = 1$ in (14), and $k_\lambda = 1000, K_z = 1000$ in (30). Note that ϵ determines the ultimate bound on heading angle error. Also, k_N determines the rate of convergence of θ_N to θ_{ref} . The gains k_1 and k_2 have influence on the ultimate bound of ϕ_0 . Finally, k_λ and K_z determine the rate of convergence and ultimate bound of Δv_t . The simulation results show that the snake robot follows the desired direction while the forward and normal velocities converge to small neighborhoods of the desired values. Figure 3 depicts the snake robot at $t = 0, 30, 60$ seconds, respectively. Figure 4 depicts the dynamic variable ϕ_0 . Figure 5 depicts the dynamic variable $\dot{\lambda}$. Figure 6 depicts the shape variable error. Figure 7 depicts the tangential and normal velocities. Finally, Figure 8 depicts the head angle of the snake robot. Note that the VHC error in Figure 6 and the head angle in Figure 8 converge faster to their steady state values because they are the first control specifications that we enforce.

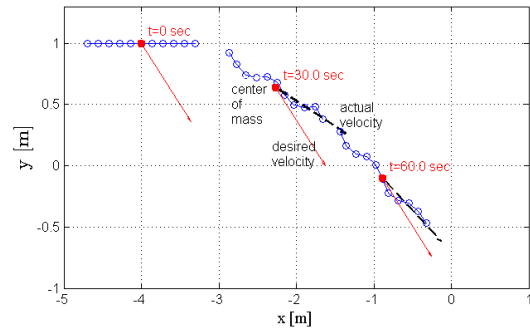


Fig. 3. Plots of the snake robot with 10 links.

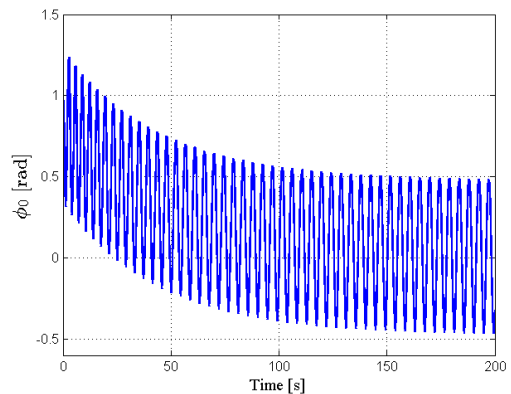


Fig. 4. The dynamic variable ϕ_0 remains uniformly ultimately bounded.

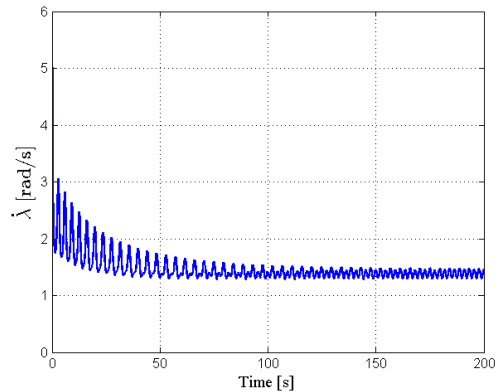


Fig. 5. The dynamic variable $\dot{\lambda}$ remains uniformly ultimately bounded.

VIII. CONCLUSIONS

We considered the problem of direction following control for a planar snake robot. We defined $N - 1$ constraint functions for directly actuated shape variables of the robot. These constraint functions were dependent on the variations of the states of dynamic compensators which were used to control the head angle and the forward velocity of the robot on the constraint manifold. Being able to control the velocity of the center of mass of the snake robot opens avenues for future research. In particular, one may use the developed technique in this paper to solve the maneuvering problem

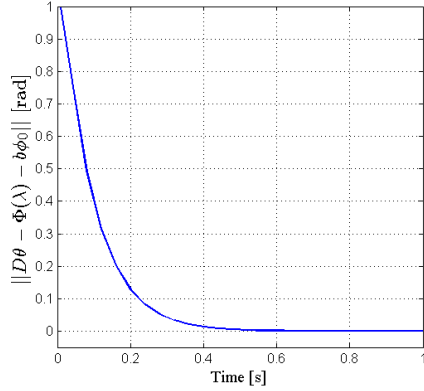


Fig. 6. The lateral undulatory gait (9) is stabilized among the shape variables of the snake robot.

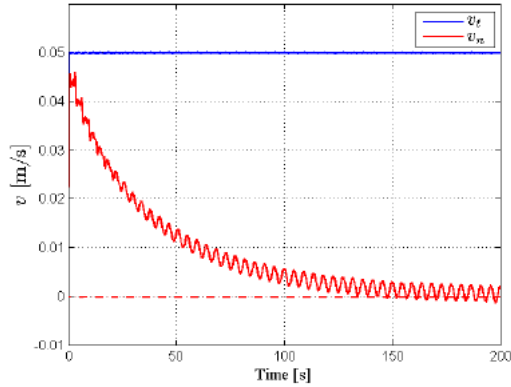


Fig. 7. Tangential and normal velocities.

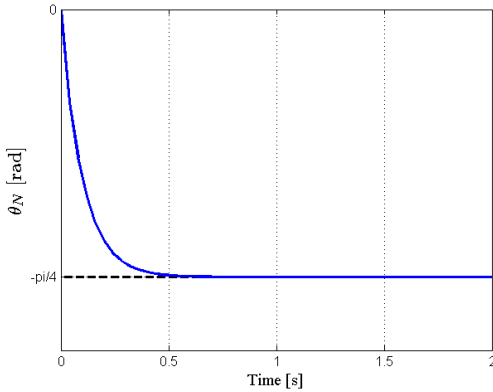


Fig. 8. The head angle of the robot.

for the snake robot. This idea will be the subject of future work.

REFERENCES

- [1] S. Hirose, *Biologically Inspired Robots: Snake-Like Locomotors and Manipulators*. Oxford University Press, 1993.
- [2] C. Ye, S. Ma, B. Li, and Y. Wang, "Turning and side motion of snake-like robot," in *IEEE International Conference on Robotics and Automation*, vol. 5. IEEE, 2004, pp. 5075–5080.
- [3] M. Sato, M. Fukaya, and T. Iwasaki, "Serpentine locomotion with robotic snakes," *IEEE Control Systems Magazine*, vol. 22, no. 1, pp. 64–81, 2002.
- [4] A. Crespi, A. Badertscher, A. Guignard, and A. J. Ijspeert, "Amphibot i: an amphibious snake-like robot," *Robotics and Autonomous Systems*, vol. 50, no. 4, pp. 163–175, 2005.
- [5] P. Liljebäck, I. U. Haugstuen, and K. Y. Pettersen, "Path following control of planar snake robots using a cascaded approach," *IEEE Trans. Control Syst. Tech.*, vol. 20, no. 1, pp. 111–126, 2012.
- [6] E. Rezapour, K. Y. Pettersen, P. Liljebäck, J. T. Gravdahl, and E. Kelasidi, "Path following control of planar snake robots using virtual holonomic constraints: theory and experiments," *Robotics and Biomimetics, SpringerOpen*, 2014.
- [7] K. A. McIsaac and J. P. Ostrowski, "Motion planning for anguilliform locomotion," *IEEE Trans. Robot. Autom.*, vol. 19, no. 4, pp. 637–652, 2003.
- [8] G. Hicks and K. Ito, "A method for determination of optimal gaits with application to a snake-like serial-link structure," *IEEE Trans. Automat. Contr.*, vol. 50, no. 9, pp. 1291–1306, 2005.
- [9] E. Cappel, M. Travers, and H. Choset, "Head-orientation for a sidewinding snake robot using modal decomposition," in *SPIE Defense+ Security*. International Society for Optics and Photonics, 2014, pp. 90 840K–90 840K.
- [10] J. Nakanishi, T. Fukuda, and D. E. Koditschek, "A brachiating robot controller," *IEEE Trans. Robot. Autom.*, vol. 16, no. 2, pp. 109–123, 2000.
- [11] F. Plestan, J. W. Grizzle, E. R. Westervelt, and G. Abba, "Stable walking of a 7-DOF biped robot," *IEEE Trans. Robot. Autom.*, vol. 19, no. 4, pp. 653–668, 2003.
- [12] A. Shiriaev, J. W. Perram, and C. Canudas-de Wit, "Constructive tool for orbital stabilization of underactuated nonlinear systems: Virtual constraints approach," *IEEE Trans. Automat. Contr.*, vol. 50, no. 8, pp. 1164–1176, 2005.
- [13] M. Maggiore and L. Consolini, "Virtual holonomic constraints for Euler-Lagrange systems," *IEEE Trans. Automat. Contr.*, vol. 58, no. 4, pp. 1001–1008, 2013.
- [14] P. Liljebäck, K. Y. Pettersen, Ø. Stavdahl, and J. T. Gravdahl, *Snake Robots: Modelling, Mechatronics, and Control*. Springer, 2013.
- [15] H. K. Khalil, *Nonlinear Systems*. Prentice Hall, 3rd edn., 2002.
- [16] M. Krstic, I. Kanellakopoulos, P. V. Kokotovic *et al.*, *Nonlinear and adaptive control design*. John Wiley & Sons New York, 1995, vol. 8.